Int. J. Electrochem. Sci., 7 **(2012)** 2374 - 2388

International Journal of
ELECTROCHEMICAL
SCIENCE
www.electrochemsci.org

Corrosion of Duplex Stainless Steel Alloy 2209 in Acidic and Neutral Chloride Solutions and its Passivation by Ruthenium as an Alloying Element

El-Sayed M. Sherif

Center of Excellence for Research in Engineering Materials (CEREM), College of Engineering, King Saud University, P. O. Box 800, Al-Riyadh 11421, Saudi Arabia
*E-mail: esherif@ksu.edu.sa

Received: 13 January 2012 / *Accepted:* 28 January 2012 / *Published:* 1 March 2012

In this work, the corrosion of duplex stainless steel (DSS) alloy 2209 alloy in 2 M HCl and 0.6 M NaCl solutions was studied. The effect of adding ~ 0.3% ruthenium (Ru) as an alloying element on the corrosion passivation of DSS in the solutions under investigation was also reported. The work has been performed using conventional gravimetric and electrochemical methods in addition to the electrochemical impedance spectroscopy measurements. The weight-loss data showed that the dissolution of DSS increased with increasing time and that effect remarkably decreased in the presence of Ru in the alloy. The electrochemical tests showed the presence of Ru shifted the corrosion potential in the positive direction and decreased the corrosion current density and both the uniform and pitting corrosion, while increased the polarization resistance of the DSS alloy. Electrochemical impedance spectroscopy revealed that the Ru alloyed DSS had higher surface and polarization resistances. The results together were internally consistent with each other, showing clearly that the presence of Ru in DSS alloy 2209 increases its passivity against corrosion in acidic and neutral chloride solutions.

Keywords: chloride media; corrosion passivation; duplex stainless steel; electrochemical tests; gravimetric data; ruthenium addition

1. INTRODUCTION

Duplex stainless steels (DSSs) are the newest in the stainless steels family and work hardenable alloys with a superior corrosion resistance to most corrosive environments. DSSs microstructures have two phases that consist of grains of ferritic and austenitic stainless steel, for which they are named duplex [1-3]. This combination of properties can mean some compromise when compared with pure austenitic and pure ferritic grades. DSSs are in most cases, tougher than ferritic stainless steel and their strengths can in some cases be double that for austenitic stainless steels [4,5]. In addition, they are nonhardenable by heat treatment, have good weldability, and excellent corrosion resistance, especially in oxidizing media and conditions conducive to localized corrosion [3-7]. These properties also allow them to be used in many applications, as example; oil and gas refining, pulp and paper manufacturing, marine environments, transport and storage, oil and gas exploration and offshore rigs, pollution control equipment, and chemical process plant [8-10].

Although, DSSs are extremely corrosion resistant alloys, corrosion can occur in different types in structures made of them while in service, especially in chloride containing media [3,5,7]. It has been reported [11-16] that these alloys suffer chloride stress cracking, fatigue crack, intergranular, pitting, and weld decay. The higher chromium and molybdenum contents increase the DSSs corrosion resistance to pitting, crevice and chloride stress corrosion cracking [8]. The corrosion resistance of virtually all stainless steels was found to increase by alloying them with minor additions of platinum group metals (PGMs) [2,9]. It has been also reported [9,17,18] that sufficient amounts of these metals retard the anodic dissolution of steels to which they are added and also increase the effectiveness of cathodic processes owing to the reduced overvoltage of hydrogen on them. The effect of two elements from PGMs, namely palladium (Pd) and ruthenium (Ru) have attracted the attention of many investigators [1,5,7,9,19-22] due to the spontaneous passivation processes of steels containing small amounts of these components. The effect of minor additions of Ru on the passivation of DSSs in 10% H2SO4 [1] and 40% H2SO4 [23] solutions were found to inhibit the anodic dissolution when active corrosion takes place. This is because Ru, if present in these alloys, acts as a blocking agent, which decreases the dissolution rates of Cr and Fe through the formation of a stable passive layer of Cr2O3 and Fe3O4 on the surface of the DSS alloy [1,5,19].

The objective of the current study was to report the corrosion of DSS alloy 2209 in 2M HCl and 0.6 M NaCl solutions. The aim was also extended to study the effect of adding circa 0.3% Ru to the DSS alloy on the passivation of its corrosion behavior in the aforementioned media. The study has been carried out in open to air solutions at room temperature using a collection of conventional and nonconventional measurement techniques. These were gravimetric weight-loss, cyclic potentiodynamic polarization, and chronoamperometric current-time at constant potential and open-circuit potential measurements along with electrochemical impedance spectroscopy investigations.

2. EXPERIMENTAL DETAILS

Two duplex stainless steel (DSS) alloys were used in this study. The first was DSS 2209 alloy with a nominal composition of Fe - 22%Cr - 9%Ni - 3%Mo. The second alloy had the same chemical compositions and cathodically modified with circa 0.3% Ru. These two alloys were prepared in a Leybold Heraeus vacuum furnace from electrolytic iron, chromium, ferromolybdenum, and nickel, as well as sponge ruthenium, under an argon atmosphere. After degassing of the raw material in a magnesia crucible, the temperature of the charge was increased to between 1610 ºC and 1670 ºC, and the molten material was cast into a steel mold. Rectangular ingots of between 3 and 5 kg were produced in each case. After cooling, samples were taken to check the bulk homogeneity. The alloys were hot-rolled from an original thickness of about 45 mm to between 3 and 5 mm. Rolling took place in a series of stages of a maximum of three passes at a time before reheating the ingot, until the desired thickness was obtained. The thermomechanical conditions chosen corresponded closely with those used for commercial SAF 2205 duplex stainless steel, and no particular difficulties were experienced in the manufacturing process.

Hydrochloric acid (HCl, Merck, 32%), sodium chloride (NaCl, Merck, 99%), were used as received. An electrochemical cell with a three-electrode configuration was used; the DSS alloys, a platinum foil, and an Ag/AgCl electrode (in 3M KCl) were used as working, counter, and reference electrodes, respectively. The DSS working electrode had rectangular dimensions of 1 x 1 x 0.4 cm, with total exposed area of 1 cm^2. These electrodes were first polished successively with metallographic emery paper of increasing fineness of up to 1000 grit then washed with doubly distilled water, degreased with acetone, washed using doubly distilled water again and finally dried with tissue paper.

The weight-loss experiments were carried out using cylindrical DSS coupons having dimensions of 1.5 cm diameter and 0.3 cm height with a total exposed area of 4.95 cm^2. The coupons were polished and dried in the same way as the DSS electrodes were, weighed (m1), and then suspended in 200 cm^3 solutions of 2 M HCl and 0.6 M NaCl for different exposure periods varied from 6 hours to 20 days. At the end of each run, the samples were rinsed with distilled water, cleaned with acetone, dried and weighed again (m^2). All weight-loss measurements were performed in triplicate and the maximum standard deviation in the observed weight loss was ± 1.5%.

Electrochemical experiments were performed by using a Potentiostat-Galvanostat 2273 (PARC Parstat-2273) Advanced Electrochemical System. The cyclic potentiodynamic polarization (CPP) experiments in 2 M HCl solutions were carried out by scanning the potential from -0.80 V and swept in the positive direction up to 1.0 V at a scan rate of 0.003 V/s; the potential was also continued sweeping from 1.0 V in the backward direction with the same scan rate. The CPP curves in 0.6 M NaCl solutions were acquired by scanning the potential from -1.2 V in the positive direction up to 0.5 V and again in the back scan direction with the same scan rate as for DSS alloys in HCl solutions. Chronoamperometric current-time experiments were carried at 0.10 V vs. Ag/AgCl as a constant potential. EIS spectra for DSSs in HCl and NaCl solutions were collected at open-circuit potentials after 1h of the alloy immersion in the test electrolyte over a frequency range of 100 kHz – 0.05 Hz, with an ac wave of ±5 mV peak-to-peak overlaid on a dc bias potential. The impedance data were collected using Powersine software at a rate of 10 points per decade change in frequency. The Nyquist plots of the EIS were fitted to an equivalent circuit model using ZSimpWin software version 3.10.

3. RESULTS AND DISCUSSION

3.1. Gravimetric weight-loss measurements

The dissolution rate (Δm, mg/cm^2) vs. time that was obtained from the weight-loss data for DSS alloy 2209 containing (1) 0.0% Ru and (2) 0.3% Ru in (a) 2 M HCl and (b) 0.6 M NaCl solutions, respectively are shown in Fig. 1. The values of Δm were calculated as follows,

$$\Delta m = \frac{m_i - m_f}{A} \qquad (1)$$

Where, mi and mf are the weighs of the DSS coupon per milligram before and after its immersion in the test solution, respectively and A is the area of the DSS coupon per cm^2. It is seen from Fig. 1 (curves 1) that the values of Δm linearly increased with time for the Ru free DSS alloy. This is due to the continuous dissolution of DSS surface in the test solution. It is also seen that although the immersion time for DSS in HCl (Fig. 1a, curve 1) was ten times shorter than in NaCl (Fig. 1b, curve 1), the values of Δm for DSS coupons in HCl solutions were much higher, nearly ten times, than that recorded for DSS in NaCl solutions. This can be attributed not only to the higher concentration of HCl compared to NaCl but also to the nature and types of reactions occur on the DSS surface in both media. Where, in HCl solutions, the cathodic reaction for DSS undergoes hydrogen evolution as follows [3,5];

$$2H^+ + 2e^- = H_2 \qquad (2)$$

On the other hand, the cathodic reaction in an open to air NaCl solutions is the reduction of oxygen according to the following equation [7],

$$2H_2O + O2 + 4e^- = 4OH^- \qquad (3)$$

The produced hydrogen gas (Eq. 2) leaves the acid solutions allowing further reaction and consuming more electrons, while the formed hydroxide groups in NaCl solutions might adsorb on the DSS surface to decrease the reaction rate.

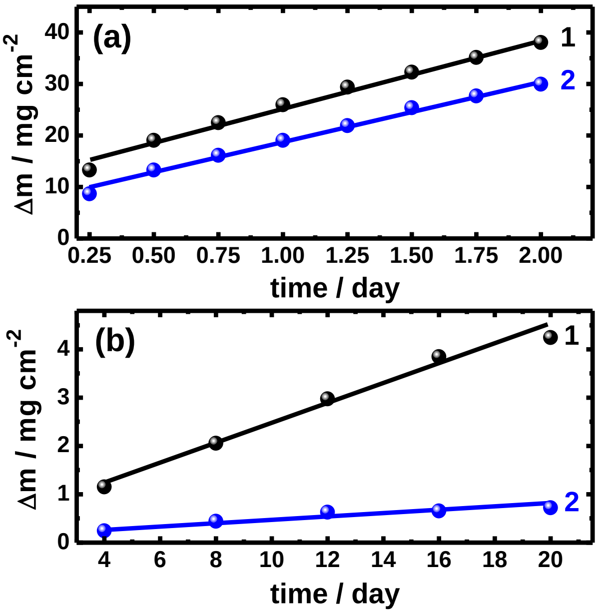

Figure 1. The relation between dissolution rate (Δm) and time for DSS 2209 alloy containing (1) 0.0% Ru and (2) 0.3% Ru in (a) 2 M HCl and (b) 0.6 M NaCl solutions, respectively.

It is generally accepted that the anodic reaction of steel in acidic and neutral chloride solutions is the dissolution of iron as can be represented by the following reaction,

$$Fe = Fe^{2+} + 2e^{-} \qquad (4)$$

The cathodic reactions consume the electrons produced by this anodic reaction as a result of the hydrogen evolutions and oxygen ions reduction. These two cathodic reactions are greatly decreased in the presence of Ru (curves 2), which is in fact led to decreasing the dissolution rate of the alloy. This is also perhaps due to the increase of the DSS corrosion resistance to chloride media by the Ru as an alloying element. According to Tomashov et al. [24], one of the reasons for the better resistance of the Ru-containing alloy was due to the fact that a large fraction of the accumulated Ru was not present in the form of an independent phase, but was included in the composition of hydroxide and oxide layers that had formed on the surface of the alloy, thereby increasing the resistance of these layers. It has been also reported [9,25,26] that the composition and morphology of the passive surfaces of the cathodically modified alloys with low concentrations of Ru confirm that the chloride ion tends to produce a coarser distribution, thus supporting the suggestion that the chloride ion increases the rate of surface diffusion of Ru during selective dissolution.

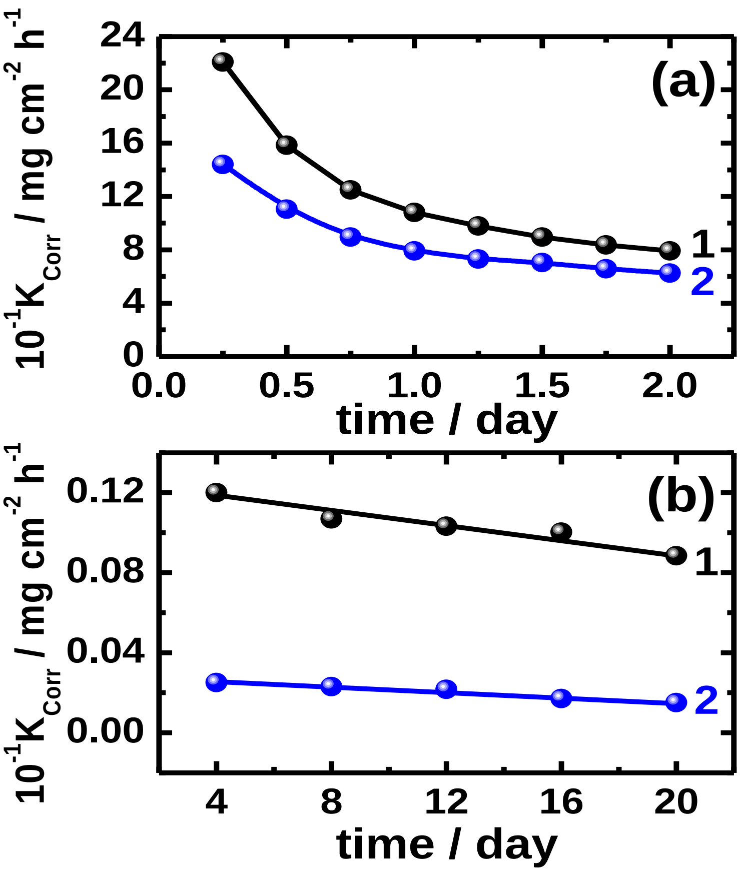

Figure 2. The change of corrosion rate (KCorr) as a function of time for DSS 2209 alloy containing (1) 0.0% Ru and (2) 0.3% Ru in (a) 2 M HCl and (b) 0.6 M NaCl solutions, respectively.

Fig. 2 shows the calculated corrosion rate (KCorr, mg cm^{-2} h^{-1}) from weight-loss data as a function of time over varied exposure time from 6 hours to 20 days for the DSS coupons without Ru (1) and with 0.3% Ru (2) in 200 ml of (a) 2M HCl and (b) 0.6 M NaCl solutions, respectively. The values of KCorr over the experimental time were calculated as follows [27-34],

$$K_{\text{Corr}} = \frac{m_i - m_f}{At} \qquad (5)$$

Here, t is the time in hours, mi, mf, and A are defined previously in Eq. (1). Although we have seen from Fig. 1 that the weight-loss, Δm, increased with time, the values of K_{Corr} decreased for both DSS alloys in the chloride media, Fig. 2. This can be explained on a general basis that metals and alloys that suffer uniform corrosion, which is characterized by a fast dissolution rate when the materials are exposed to the corrosive media. Increasing the immersion time of those materials decreases the uniform corrosion due to the formation of top layers of corrosion products and/or oxide films, especially in NaCl solutions. These corrosion products are not compact enough and only produce partial protection if it stays on the alloy surface. It is also seen from Fig. 2 that the presence of Ru, curves 2, to a great extent decreased the values of K_{Corr} over the whole experimental exposure time. This is due to the fact that Ru at this low content has the ability to increase the passivation of the DSS surface and thus decreases the aggressiveness of the chloride ions attack.

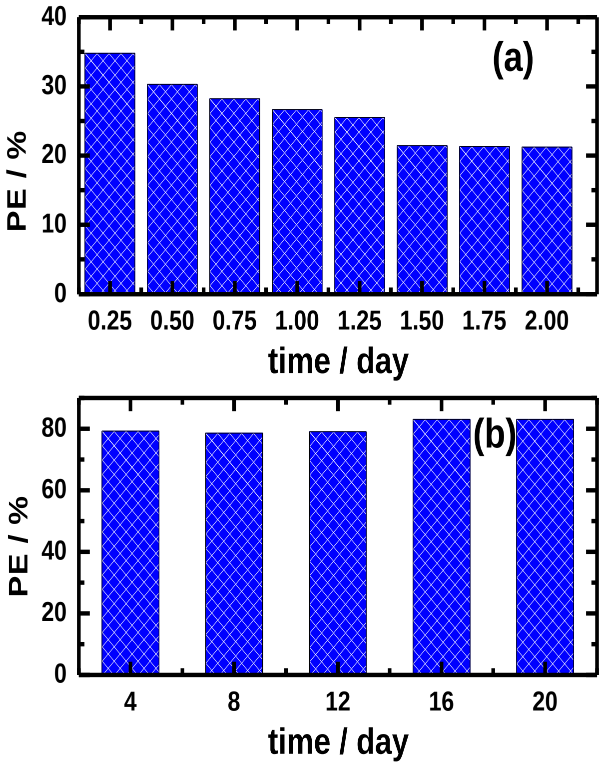

Figure 3. Change of the PE% as a function of time for DSS alloy by 0.3% Ru in (a) 2M HCl and (b) 0.6 M NaCl solutions, respectively.

In order to confirm the ability of Ru on the protection of DSS alloy 2209 against corrosion in HCl and NaCl solutions, the values of the passivation efficiency (*PE%*) of the DSS by Ru were calculated as the case of inhibition efficiency as follows [35-41];

$$PE\% = \frac{K^{1}_{Corr} - K^{2}_{Corr}}{K^{1}_{Corr}} \, x \, 100 \qquad (6)$$

Where K^{1}_{Corr} and K^{2}_{Corr} are the corrosion rates calculated using Eq. (5) for the DSS alloy in the absence and presence of Ru, respectively. The change of PE% as a function of time for the DSS alloy by 0.3% Ru in (a) 2 M HCl and (b) 0.6 M NaCl solutions is shown in Fig. 3.

The passivation efficiency of DSS alloy by Ru in HCl solutions recorded circa 35% after 6 hours decreased to about 22% in 2 days. On the other hand, the PE% was about 80% increased to circa 82% in 20 days. The difference in PE% values obtained for HCl than NaCl is due to the higher corrosiveness action of acid compared to the neutral NaCl solutions. This might be due to the role of Ru in the formation of a thin, compact film on the alloy surface [9,22,42]; this possibility is higher to occur in NaCl than in HCl solutions. It has been reported [22,42,43] that the presence of Ru in the DSS alloy leads to a possible Ru interaction effect with Fe that leads to the formation of Fe_3O_4 and allows the free diffusion of Cr to the surface to form Cr_2O_3, which could decrease the weight-loss and corrosion rate of the DSS alloy under investigation.

3.2. Cyclic potentiodynamic polarization (CPP) measurements

In order to report the corrosion and corrosion passivation in the chloride solutions of the DSS alloy in the absence and presence of Ru, the CPP measurements were carried out. The CPP curves for the DSS alloy containing (1) 0.0% Ru and (2) 0.3% Ru in (a) 2M HCl and (b) 0.6 M NaCl solutions are shown in Fig. 4. It is clearly seen that the anodic branch for the DSS alloys shows an active-passive region.

The active region is probably due to the dissolution of iron from the alloy as represented by Eq. (4). On the other hand, the passive region is perhaps as a result of the formation of corrosion products and/or oxide film on the DSS alloy surface, where the current decreased to show a large passive area with increasing potential.

Increasing the potential in the more positive direction in HCl solutions, Fig. 4a (curve 1), resulted in a complete dissolution and breakdown of the formed passive film, which could led to the rapid increase of current values.

While, in NaCl solutions, Fig. 4b, curve 1) the current increased slightly with potential and the breakdown of the formed passive film was not clear.

Back scanning the potential for the DSS alloy that had no Ru (Fig. 4, curves 1) produced higher currents than those obtained from the forward ones, which indicates on the occurrence of pitting corrosion.

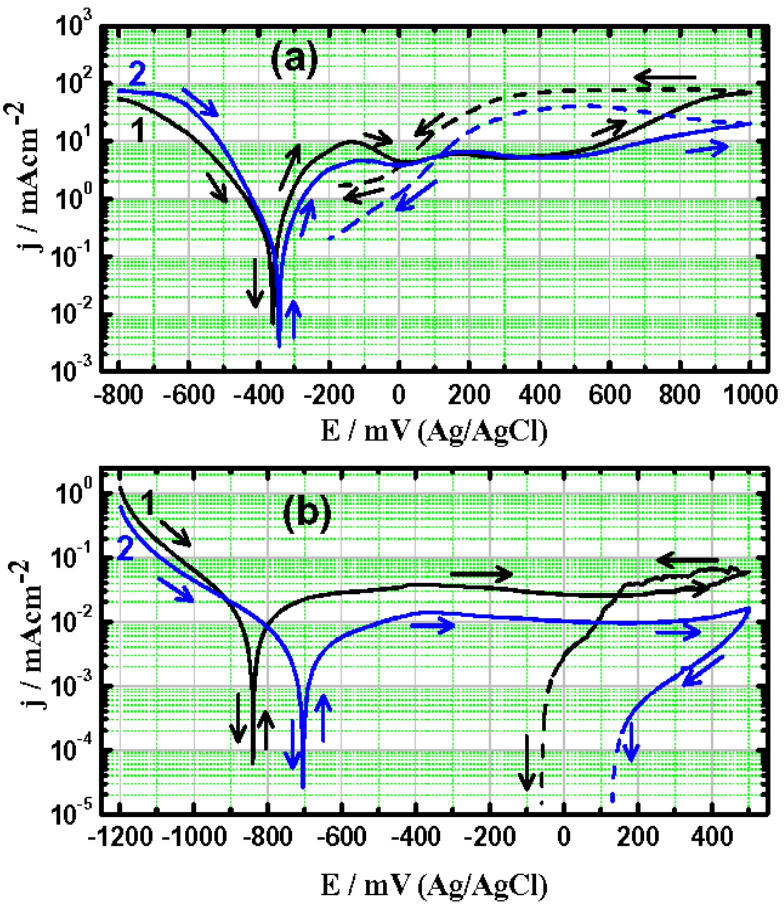

Figure 4. Cyclic potentiodynamic polarization curves obtained for DSS 2209 alloy containing (1) 0.0% Ru and (2) 0.3% Ru in (a) 2 M HCl and (b) 0.6 M NaCl solutions, respectively.

The CPP curves for DSS alloy containing Ru (Fig. 4, curves 2) showed similar behavior but with significant lower cathodic, anodic and corrosion current density (j_{Corr}), a less negative shift in the corrosion potential (E_{Corr}) values. The pitting corrosion was also noticed in HCl solution as the reverse currents were higher than the forward values to form a hysteresis loop but with a smaller area compared to DSS alloy having no Ru. This was not the case for DSS/0.3% Ru in NaCl solutions, where the curve did not show any hysteresis loop that means the pitting corrosion did not occur at this condition.

Table 1. Parameters obtained from CPP curves shown in Fig. 4for the DSS alloys in 2M HCl and 0.6 M NaCl solutions.

Alloy	Parameter						
	E_{Corr}/ mV	βc/ mVdec^{-1}	βa/ mVdec^{-1}	j_{Corr}/ µAcm^{-2}	Rp /Ωcm^2	K_{Corr}/ mmpy	PE/ %
DSS/0.0%Ru HCl	-370	70	100	230	78.00	0.660	–
DSS/0.3%Ru HCl	-338	95	120	115	46.00	0.330	50.00
DSS/0.0%Ru NaCl	-929	95	140	7.6	3240	0.022	–
DSS/0.3%Ru NaCl	-897	120	160	2.5	11920	0.007	67.10

The values of the cathodic (βc) and anodic (βa) Tafel slopes, j_{Corr}, E_{Corr}, polarization resistance (R_P), corrosion rate (K_{Corr}), and percentage of the passivation efficiency (PE%) obtained from Fig. 4 are listed in Table 1. The values of j_{Corr} and E_{Corr} were obtained from the extrapolation of anodic and cathodic Tafel lines located next to the linearized current regions [45-52]. The R_P and K_{Corr} values were also calculated as reported in our previous studies [45-52]. The values of PE% were obtained as in the case of the inhibition efficiency as follows [35-41],

$$PE\% = \frac{j_{Corr}^{1} - j_{Corr}^{2}}{j_{Corr}^{1}}\ x\,100 \tag{7}$$

Here j_{Corr}^{1} and j_{Corr}^{2} are the corrosion currents for the DSS alloys in the absence and presence of Ru, respectively.

The decrease in the values of jCorr and KCorr and the increase of RP, and PE% in the presence of 0.3% Ru are mainly due to the increased surface resistance of the DSS against general and pitting attacks. The positive shift in the *ECorr* and also the increases in the *βc* and *βa* values are mainly due to decreasing the general dissolution and pitting corrosion of the alloy through decreasing the rate of the anodic and cathodic reactions [9,20]. The CPP results thus are in very good agreement with those obtained from gravimetric data; both indicated that the presence of Ru increases the passivation of the DSS surface against corrosion.

3.3. Chronoamperometric current-time measurements

The chronoamperometric current-time experiments were carried out for DSS alloys in chloride solutions, in order to study whether pitting corrosion occurs and to shed more light on the effect of Ru on the passivation of DSS alloy. The variation of the dissolution currents of the DSS alloy 2209 without (1) and with 0.3% Ru (2) versus time at 0.10 V vs. Ag/AgCl in (a) 2M HCl and (b) 0.6 M NaCl solutions, respectively are shown in Fig. 5. One can see from Fig. 5a (curve 1) that the current increased then decreased in the first few seconds to reach its minimum after about 100 sec. The current then increased linearly with time till end of the run. This is probably due to the dissolution of the alloy surface and the occurrence of pitting corrosion. While, the presence of Ru, Fig. 5a (curve 2), decreased the initial current to record few microamperes. Increasing the time of the experiment slightly increased the current. The high absolute current and the increase of its value with time in the absence of Ru indicate that the alloy suffers both uniform and pitting corrosion. On the other hand, the presence of Ru decreased the current values to its minimum over the exposure time, which proves that Ru to a great extent is able to protect the DSS alloy against corrosion in 2 M HCl solutions.

The current of DSS alloys in NaCl solutions, Fig. 5b, recorded values almost 100 times lower than that obtained in HCl solutions due to the higher aggressiveness action of HCl compared to NaCl towards the DSS alloys. Fig. 5b (curve 1) shows an increased current values with some current fluctuations recorded with increasing the time of the experiment. This behavior indicates that pitting corrosion of the alloy occurs. The presence of 0.3% Ru as shown by curve 2 (Fig. 5b) significantly lowered the absolute current to its minimum with further decreases recorded with time till end of the run. The fluctuations seen on curve 1 were also completely disappeared due to the presence of Ru. This means that alloying the DSS alloy 2209 with 0.3% Ru decreases its uniform corrosion and totally prevents its pitting corrosion in 0.6 M NaCl solution. Chronoamperometric current-time measurements thus agree with the data obtained by weight-loss and CPP experiments that adding a minor content of Ru, 0.3% provides great extent of protection to the DSS alloy 2209 against corrosion in the chloride media under investigation.

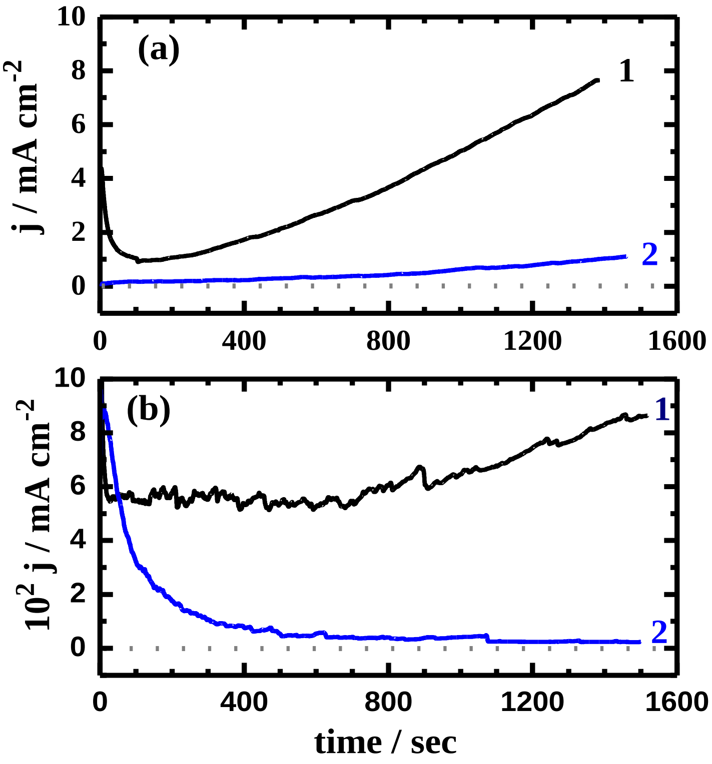

Figure 5. Chronoamperometric current-time curves obtained for DSS 2209 alloy containing (1) 0.0% Ru and (2) 0.3% Ru in (a) 2 M HCl and (b) 0.6 M NaCl solutions, respectively at 100 mV vs. Ag/AgCl.

3.4. Open-circuit potential and electrochemical impedance spectroscopy measurements

The open-circuit potential (OCP) versus time for 1h curves for the DSS alloy 2209 containing (1) 0.0% Ru and (2) 0.3% Ru in (a) 2M HCl and (b) 0.6 M NaCl solutions, respectively are shown in Fig. 6. It can clearly be seen from Fig. 6a (curve 1) that the potential of the DSS alloy decreases to the more negative values in the first few moments. This is due to the dissolution of a most probably an oxide film was formed on the alloy surface in air before being immersed in the test solution. The potential started to increase in the less negative direction again with increasing time; this increase continued to occur till the end the 1 h immersion time. This is mostly due to a chemical reaction between the acid molecules and the surface, which could lead to the formation of a top layer of corrosion products that partially decreases the dissolution of the alloy with time. The OCP of the DSS alloy containing 0.3% Ru (Fig. 6a, curve 2) showed almost similar behavior to that of the Ru free DSS but with a higher positive potential shift over the whole time of the experiment, which means that the presence of Ru provides more corrosion resistance to the DSS alloy.

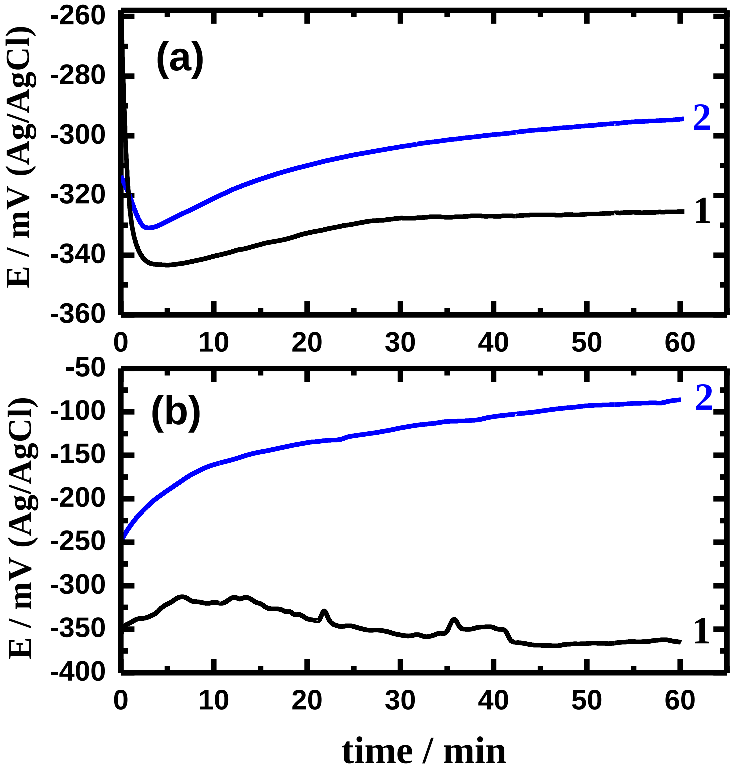

Figure 6. Variations of the open-circuit potential as a function of time for DSS alloy containing (1) 0.0% Ru and (2) 0.3% Ru in (a) 2 M HCl and (b) 0.6 M NaCl solutions, respectively.

For the Ru free DSS alloy in 3.5% NaCl solution, Fig. 6b (curve1), the OCP decreased in the less negative direction from the first moment of alloy immersion and to about 7 min; this is due to the air preformed oxide film thickening. The OCP thereafter slightly decreased to the more negative values with increasing time up to the end of the experiment as a result of the chloride ions attack to the flawed areas on the surface of the alloy. On the other hand, the OCP of the Ru containing DSS alloy, Fig. 6b (curve 2) showed an initial positive shift of about 100 mV (from -350 for DSS + 0.0Ru to -250 mV for DSS + 0.3%Ru) and continued increasing in the same direction to reach to ~ -50 mV in 1h. The initial positive shift is due to the higher corrosion resistance of the Ru containing DSS alloy compared to Ru free alloy. As well as, the continuous OCP positive shift from the first moment of immersion and across the whole run resulted due to the ability of Ru to provide high passivation status to the alloy enables it to withstand against the aggressiveness attack of the chloride ions. This agrees with previous studies [3,19], in which it was reported that stainless steels with low Ru content are passivated spontaneously due to the formation of passive layers of remarkably increased corrosion resistance on their surfaces, that shifted the corrosion potential of these alloys toward the more positive values.

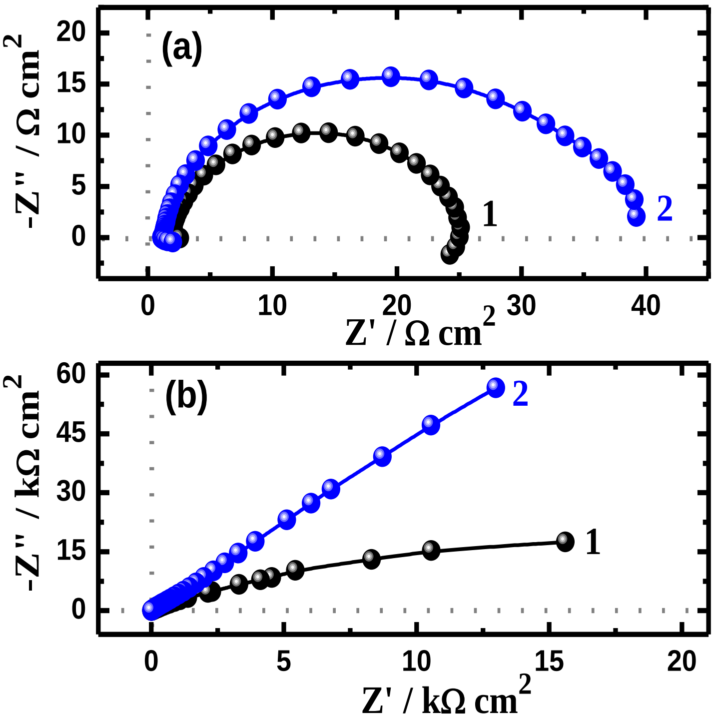

Figure 7. Typical Nyquist plots obtained for DSS 2209 alloy containing (1) 0.0% Ru and (2) 0.3% Ru after 1 hour immersion in (a) 2 M HCl and (b) 0.6 M NaCl solutions, respectively.

The electrochemical impedance spectroscopy (EIS) experiments were carried out in this study to report the obtained mechanistic and kinetic information [54-58] for the corrosion and corrosion passivation of DSS alloy 2209 without and with Ru present in the test chloride solutions. Typical Nyquist plots obtained for DSS containing (1) 0.0% Ru and (2) 0.3% Ru after 1h immersion in (a) 2 M HCl and (b) 0.6 M NaCl solutions respectively are shown in Fig. 7. The data of the plots shown in Fig. 7a and Fig. 7b were analysed by fitting its values to the two equivalent circuit models shown in Fig. 8a and Fig. 8b, respectively. The parameters obtained by fitting the equivalent circuit models are listed in Table 2. These parameters can be defined as: Rs is the solution resistance, Q is the constant phase elements (CPEs), Rp is the polarization resistance, Rp* is another polarization resistance, and L is the conductance.

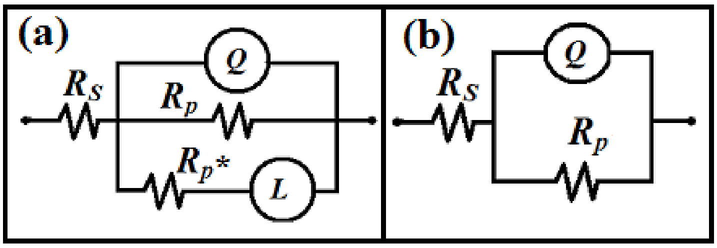

Figure 8. The equivalent circuit models (a) and (b) used to fit the EIS Nyquist plots presented in Fig. 7a and Fig. 7b, respectively.

It is clear from Fig. 7a that only single but distorted semicircles are observed for the DSS electrode regardless of whether Ru is present or not. It is also seen that the presence of Ru increased the diameter of the obtained semicircle and so increased the values of the resistances, Rs, Rp, and Rp*; this is probably due to the formation of a passive layer on the alloy surface. This increase in the resistance of both electron transfer reactions in Ru containing alloy is in general agreement with the positive shift in the corrosion potential [55-58]. The CPEs (Q) as well have characteristics similar to those of capacitors with their n values close to 1.0 in all solutions. The presence of Ru decreased the value of CPEs, which indicates that the capacitive effect decreased to cover the charged surfaces of the DSS alloy [59,60]. The presence of the inductive (*L*) loop in the circuit model of HCl solutions suggests that the passivated surface re-dissolves at low frequencies [47]. The steady decrease of *L* values indicates that the dissolution of the passive film formed on the DSS alloys decreases in the presence of Ru. The EIS results thus confirm the data obtained by weight-loss, polarization and chronoamperometric current-time measurements.

Table 2. EIS parameters obtained by fitting the Nyquist plot shown in Fig. 7a with the equivalent circuit shown in Fig. 8 for DSS alloys in 2M HCl and 0.6 M NaCl solutions.

	Parameter					
Alloy	Rs/ Ω cm^2	Q		Rp/ Ω cm^2	Rp*/ Ω cm^2	L/ H
		YQ/F μcm^{-2}	n			
DSS/0.0%Ru HCl	0.90	48.25	0.92	22.18	32.67	273
DSS/0.3%Ru HCl	1.57	30.15	0.90	39.55	37.04	0.28
DSS/0.0%Ru NaCl	7.58	1.18	0.89	42.70	–	–
DSS/0.3%Ru NaCl	12.44	0.41	0.82	172.40	–	–

4. CONCLUSIONS

The corrosion and corrosion passivation of DSS alloy 2209 in chloride media namely, 2 M HCl and 0.6 M NaCl solutions by modification with 0.3% Ru. The study has been carried out by weight-loss, polarization, chronoamperometry, open-circuit potential and electrochemical impedance spectroscopy measurements. It was found that the corrosion rate of DSS in HCl solution is higher than that obtained in NaCl. The cathodic reaction for DSS in HCl solution was hydrogen evolution but in NaCl was oxygen reduction. Therefore, the dissolution of DSS via uniform corrosion was more observed in HCl, while pitting attack was higher in NaCl solutions. Alloying DSS with Ru had a great impact on the passivation of the alloy against uniform and pitting corrosion in both solutions. Gravimetric data indicated that Ru decreases the corrosion rate and increases the passivation efficiency of the DSS alloy. Electrochemical results confirmed also that the presence of Ru shifted the corrosion potential to the more noble values, decreased the cathodic and anodic currents as well as the corrosion current density and corrosion rate. This effect also increased the surface and polarization resistances of the DSS alloy 2209 in both HCl and NaCl solutions. Both gravimetric and electrochemical results are in good agreement with each other confirm without doubt that Ru has a great ability on the passivation of DSS alloy 2209 against corrosion in an open to air solution of 2 M HCl and 0.6 M NaCl at room temperature.

ACKNOWLEDGEMENT
This project was supported by King Saud University, Deanship of Scientific Research, College of Engineering Research Center

References

1. El-Sayed M. Sherif, *Int. J. Electrochem. Sci.*, 6 (2011) 2284.
2. K. Varga, P. Baradlai, W. O. Barnard, G. Myburg, P. Halmos and J. H. Potgieter, *J. Electrochim. Acta*, 42 (1997) 25.
3. J. H. Potgieter, P. A. Olubambi, L. Cornish, C.N. Machio, El-Sayed M. Sherif, *Corros. Sci.*, 50 (2008) 2572.
4. R. Leiva-García, M. J. Muñoz-Portero, J. García-Antón, *Int. J. Electrochem. Sci.*, 6 (2011) 830.
5. El-Sayed M. Sherif, J. H. Potgieter, J. D. Comins, L. Cornish, P. A. Olubambi, C. N. Machio, *J. Appl. Electrochem.*, 39 (2009) 1385.
6. D. M. García-García, E. Blasco-Tamarit, J. García-Antón, *Int. J. Electrochem. Sci.*, 6 (2011) 1237.
7. El-Sayed M. Sherif, J. H. Potgieter, J. D. Comins, L. Cornish, P. A. Olubambi, C. N. Machio, *Corros. Sci.*, 51 (2009) 1364.
8. Z. Sun, M. Kuo, I. Annergren, D. Pan, *Mater. Sci. Eng. A*, 356 (2003) 274.
9. J. H. Potgieter, *Shreir's Corrosion*, 3 (2010) 2224.
10. C.T. Kwok, F.T. Cheng and H.C. Man, *Mater. Sci. Eng. A*, 290 (2000) 145.
11. A. Wilson, *Stainless Steel Engineering*, 2nd ed. Johnson Press London (1995) P. 45-60.
12. G.H. Aydogdu, M.K. Aydinol, *Corros. Sci.*, 48 (2006) 3565.
13. Y.Y. Chen, L.B. Chou, H.C. Shih, *Mater. Chem. Phys.*, 97 (2006) 37.
14. N. Parvathavarthini, R.K. Dayal, H.S. Khatak, V. Shankar, V. Shanmugam, *J. Nucl. Mater.*, 355 (2006) 68.
15. L. Llanes, A. Mateo, P. Violan, J. Méndez, M. Anglada, *Mater. Sci. Eng. A*, 234-236 (1997) 850.
16. L. Llanes, A. Mateo, P. Villechaise, J. Méndez., M. Anglada, *Inter. J. Fatigue*, 21 (1999) S119.
17. J.H. Potgieter, *J. Appl. Electrochem.*, 21 (1991) 471.
18. J.H. Potgieter, A.M. Heyns, W. Skinner, *J. Appl. Electrochem.*, 20 (1990) 711.
19. G. Myburg, K. Varga, W.O. Barnard, P. Baradlai, L. Tomcsânyi, J.H. Potgieter, C.W. Louw, M.J. Van Staden, *Appl. Surf. Sci.*, 136 (1998) 29.
20. J.H. Potgieter, W.O. Barnard, G. Myburg, K. Varga, P. Baradlai, L. Tomcsânyi, *J. Appl. Electrochem.*, 26 (1996) 1103.
21. S.C. Tjong, *Appl. Surf. Sci.*, 44 (1990) 7.
22. I.M. Wolff, L.E. Iorio, T. Rumpf, P.V.T. Scheers and J.H. Potgieter, *Mater. Sci. Eng. A*, 241 (1998) 264.
23. J.H. Potgieter, P. Ellis, A. Van Bennekom, *ISIJ International*, 35 (1995) 197.
24. N.D. Tomashov, G.P. Chernova, L.A. Chigirinskaya, E.A. Nasedkina, *Prot. Met.*, 22 (1986) 704.
25. H.W. Pickering, *Corros. Sci.*, 23 (1983) 1107.
26. A. Higginson, R.C. Newman, R.P.M. Proctor, *Corros. Sci.*, 29 (1989) 1293.
27. El-Sayed M. Sherif, R.M. Erasmus, J.D. Comins, *Corros. Sci.*, 50 (2008) 3439.
28. El-Sayed M. Sherif, R.M. Erasmus, J.D. Comins, *J. Appl. Electrochem.*, 39 (2009) 83.
29. El-Sayed M. Sherif, *Int. J. Electrochem. Sci.*, 6 (2011) 5372.

30. El-Sayed M. Sherif, A.A. Almajid, A.K. Bairamov, E. Al-Zahrani, *Int. J. Electrochem. Sci.*, 6 (2011) 5430.
31. El-Sayed M. Sherif, A.A. Almajid, *Int. J. Electrochem. Sci.*, 6 (2011) 2131.
32. El-Sayed M. Sherif, *J. Mater. Eng. Perform.*, 19 (2010) 873.
33. El-Sayed M. Sherif, A.A. Almajid, *J. Appl. Electrochem.*, 40 (2010) 1555.
34. El-Sayed M. Sherif, A.H. Ahmed, *Synthesis and Reactivity in Inorganic, Metal-Organic and Nano-Metal Chemistry*, 40 (2010) 365.
35. El-Sayed M. Sherif, R. M. Erasmus, J. D. Comins, *Electrochim. Acta*, 55 (2010) 3657.
36. El-Sayed M. Sherif, *Int. J. Electrochem. Sci.*, 6 (2011) 1479.
37. El-Sayed M. Sherif, *Mater. Chem. Phys.*, 129 (2011) 961.
38. El-Sayed M. Sherif, *Int. J. Electrochem. Sci.*, 6 (2011) 3077.
39. El-Sayed M. Sherif, A.A. Almajid, F.H. Latif, H. Junaedi, *Int. J. Electrochem. Sci.*, 6 (2011) 1085.
40. Khalil A. Khalil, El-Sayed M. Sherif, A.A. Almajid, *Int. J. Electrochem. Sci.*, 6 (2011) 6184.
41. F.H. Latief, El-Sayed M. Sherif, A.A. Almajid, H. Junaedi, *J. Anal. Appl. Pyrol.*, 92 (2011) 485.
42. M.J. Van Staden, J.P. Roux, *Appl. Surf. Sci.*, 44 (1990) 263.
43. S.C. Tjong SC, W.O. Barnard, J.B. Malherbe, *J. Mater. Sci.*, 27 (1992) 1818.
44. P. Baradlai, J.H. Potgieter, W.O. Barnard, L. Tomcsanyi, K. Varga, Mater. Sci. Forum, 185(1995)188.
45. E.M. Sherif, S.-M. Park, *J. Electrochem. Soc.*, 152 (2005) B205.
46. E.M. Sherif, S.-M. Park, *Electrochim. Acta*, 51 (2006) 1313.
47. E.M. Sherif, S.-M. Park, *Electrochim. Acta*, 51 (2006) 4665.
48. El-Sayed M. Sherif, *J. Appl. Surf. Sci.*, 252 (2006) 8615.
49. E.M. Sherif, S.-M. Park, *J. Electrochem. Soc.*, 152 (2005) B428.
50. E.M. Sherif, S.-M. Park, *Electrochim. Acta*, 51 (2006) 6556.
51. E.M. Sherif, S.-M. Park, *Corros. Sci.*, 48 (2006) 4065.
52. El-Sayed M. Sherif, A.M. El Shamy, M.M. Ramla, A.O.H. El Nazhawy, *Mater. Chem. Phys.*, 102
53. (2007) 231.
54. J.R. Macdonald, *Impedance Spectroscopy*, John Wiley & Sons, New York, 1987.
55. F. Mansfeld, S. Lin, S. Kim, H. Shih, *Corros. Sci.*, 27 (1987) 997.
56. El-Sayed M. Sherif, R. M. Erasmus, J. D. Comins, *J. Colloid Interface Sci.*, 306 (2007) 96.
57. El-Sayed M. Sherif, R. M. Erasmus, J. D. Comins, *J. Colloid Interface Sci.*, 309 (2007) 470.
58. El-Sayed M. Sherif, R. M. Erasmus, J. D. Comins, *J. Colloid Interface Sci.*, 311 (2007) 144.
59. L. Larabi, Y. Harek, O. Benali, S. Ghalem, *Prog. Org. Coat.*, 54 (2005) 256.
60. A. Popova, E. Sokolova, S. Raicheva, M. Christov, *Corros. Sci.*, 45 (2003) 33.